

Deformation of *In-Situ*-Reinforced Bulk Metallic Glass Matrix Composites

B. Clausen¹, S.-Y. Lee¹, E. Üstündag^{1,*}, C. P. Kim¹,
D. W. Brown² and M. A. M. Bourke²

¹ California Institute of Technology, Department of Materials Science, M/C 138-78, Pasadena, CA 91125, USA

² Los Alamos National Laboratory, Materials Science and Technology Division, MS H805, Los Alamos, NM 87545, USA

Keywords: Bulk metallic glass, composite, *in-situ* loading, neutron diffraction, self-consistent modeling.

Abstract. Bulk metallic glasses (BMGs) are potentially superb structural materials due to a unique combination of properties such as a large elastic strain limit, high strength and good fracture toughness. However, most BMGs are prone to catastrophic failure during unconstrained loading due to high concentration of shear deformation in the form of a shear band. This problem has been addressed by the development of BMG-matrix composites that suppress this failure mode. In this study we have utilized neutron diffraction measurements to investigate the load sharing in such a BMG-matrix composite, where the second phase is formed *in-situ* during quenching. The properties of the second phase itself have also been investigated in the monolithic form. The diffraction data has been compared to the predictions of self-consistent models resulting in good agreement.

Introduction

Bulk metallic glasses (BMGs) have recently gained attraction as structural materials due to their very large elastic strain limit, about 2%, high strength (over 2 GPa) and a good fracture toughness, up to 55 MPa m^{1/2} [1, 2, 3]. However, most BMGs are prone to catastrophic failure during unconstrained loading, which severely limits their use in structural applications.

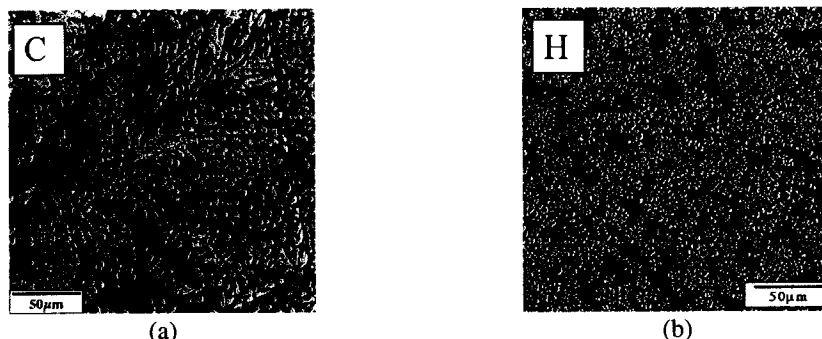


Figure 1. SEM backscattered electron images of the microstructure of two different *in-situ* BMG composites, from [8]: (a) produced at Caltech; (b) produced at Howmet Corp. The light regions are the β phase while the dark gray indicates the BMG matrix. These microstructures indicate that the scale of the β phase dendrites can be varied by using different casting procedures. This allows for microstructure, and hence, property control.

* Corresponding author; e-mail: ersan@caltech.edu.

This problem has been addressed by the development of several BMG-matrix composites that suppress this failure mode [4, 5, 6, 7]. The most promising of these BMG composites are obtained *in situ* as the reinforcements precipitate out during casting [8, 9]. These composites consist of a BMG matrix with a fine dendritic second phase. The second phase has a BCC crystal structure, consists of primarily Zr and Ti and hence is referred to as the “ β phase” since it is similar to the β phase of both Ti and Zr (their “ α phase” at room temperature is HCP). The interpenetrating/dendritic structure of the β phase (see Fig. 1) has been shown to inhibit the formation of macroscopic shear bands in the matrix which cause catastrophic failure in monolithic BMGs. The mechanical properties of the BMG/ β phase composites have previously been characterized using macroscopic measurements such as ultrasonic methods to determine elastic constants, conventional tension/compression and Charpy-impact testing [8]. In the present study, we have used neutron diffraction, aided by self-consistent modeling, to characterize the load partitioning in the composites and the deformation behavior of the monolithic β phase alloy during uniaxial compression.

The neutron diffraction technique allows for *in-situ* bulk measurements of internal strains in crystalline materials [10] and is ideal for composite systems as it is phase specific [11, 12]. However, in the case of BMG, the amorphous structure does not give rise to Bragg peaks. Although it is possible to extract structural information about the BMG from its neutron diffraction signature using pair distribution function analysis [13], in this study we have chosen to investigate BMG-based composites with a crystalline second phase. This way we could utilize the second phase as an “internal strain gauge”, and by combining the measurements with model predictions for the composite behavior, we could infer the *in-situ* behavior of the BMG indirectly. The other advantage of neutron diffraction is that the high average atomic number of the BMG alloy precludes the use of X-ray diffraction whereas the deep penetration of neutrons allows access to the bulk behavior of the material.

Experimental Procedure

The β phase/BMG composites were prepared using the casting procedure described in [8]. They had a microstructure similar to that shown in Fig. 1(a). Following a similar procedure, monolithic β phase specimens were also prepared having the same chemical composition as that of the β phase dendrites inside the *in-situ* BMG composites. The final sample dimensions were 5.97 (diam.) by 14.34 mm (aspect ratio, $l/d = 2.4$) and 5.84 (diam.) by 14.60 mm ($l/d = 2.5$) for the monolithic and composite samples, respectively. The relatively high aspect ratio is needed to assure an acceptable gauge volume in the diffraction measurements, see Fig. 2(a).

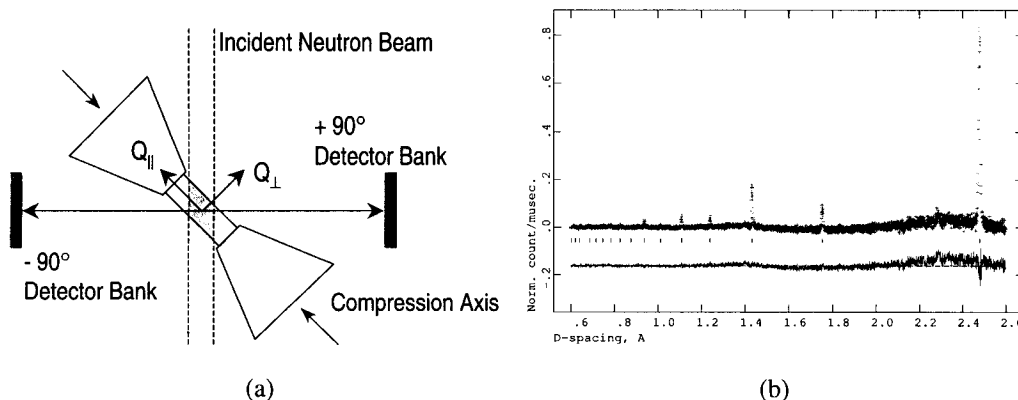


Figure 2. (a) Schematic setup of neutron powder diffraction experiments. The scattering vectors for each detector indicate the direction of lattice strain measurements relative to the loading axis. (b) Typical

diffraction pattern for a BMG/ β phase composite; symbols are measured data, the line fitting the symbols is the Rietveld refinement, and the lower line is the difference curve. The wavy background in (b) is due to the amorphous BMG matrix.

The neutron diffraction measurements were performed at the Manuel Lujan, Jr. Neutron Scattering Center, Los Alamos National Laboratory using the neutron powder diffractometer (NPD). The setup of NPD (see schematic in Fig. 2(a)) allows for collection of multiple diffraction patterns simultaneously. A load frame has been specially constructed for the instrument [14] such that scattering vectors for the two $2\theta = \pm 90^\circ$ banks are oriented parallel (\parallel) and perpendicular (\perp) to the loading axis, and thereby it is possible to measure the longitudinal and transverse elastic lattice strains in the sample simultaneously. Using the time-of-flight (TOF) technique, entire diffraction patterns are collected (see Fig. 2(b)) and the Rietveld technique [15, 16] has been employed to determine an average lattice strain in the β phase. The reported elastic lattice strains are relative to the lattice constants at a nominal 5 MPa compression needed to hold the samples in place.

Results

Diffraction data obtained from a monolith and a composite are shown in Fig. 3. It is seen that the stiffness determined from Rietveld refinements of the diffraction data for the monolithic β phase sample (M5), 59 GPa, is about 6% lower than the literature value of 63 GPa [8]. For the β phase/BMG composite sample, the effective *in-situ* Young's modulus of the β phase in the composite measured by the diffraction data is 76 GPa. Note that this is not the same as the *in-situ* stiffness of the β phase since it is obtained from the slope of the applied composite stress vs. elastic (lattice) strain.

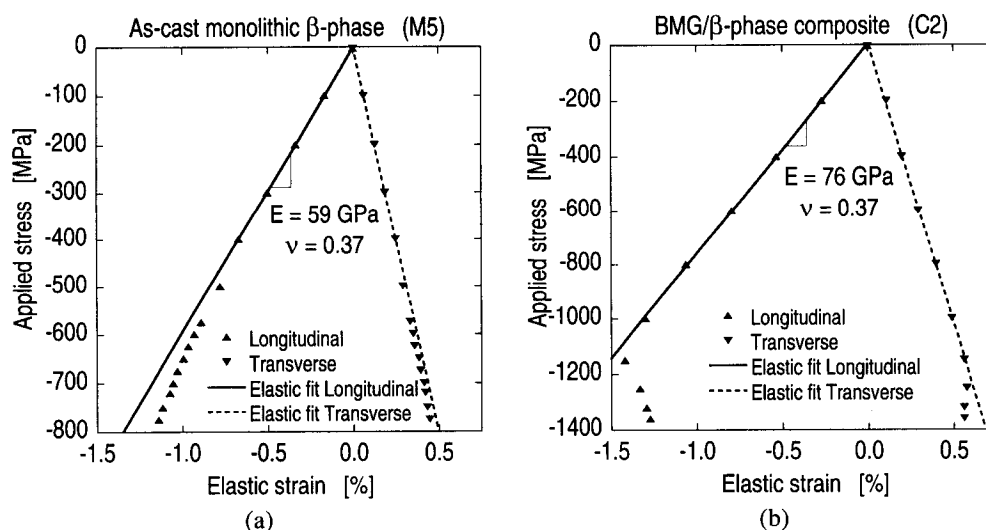


Figure 3. Measured elastic lattice strains in β phase as a function of applied stress: (a) in the monolithic sample; (b) in the BMG/ β phase composite (using Rietveld refinements).

In addition to the Rietveld refinement, we have also performed single peak fits to the (110), (200), (211), (310) and (321) reflections of the β phase. The results are shown in Fig. 4 together with predictions by the self-consistent modeling (described in the next section). As seen in Fig. 4, the single peak results show a pronounced anisotropy in the β phase, which is obvious from the wide spread of stiffnesses for individual reflections. When plasticity occurs, above -600 MPa applied stress, the peaks spread further due to the plastic anisotropy of the material. The single

peak results for the composite sample are shown in Fig. 4(b). The high anisotropy of the β phase is also observed in the composite, but as plasticity occurs, above -1100 MPa applied stress, the general trend of the peaks is more vertical than in the monolith likely due to the constraints imposed by the BMG matrix.

Modeling

Modeling of this type of composite is not trivial. The random dendritic structure of the second phase makes unit-cell finite element modeling difficult, and the assumption of ellipsoidal inclusions in Eshelby type calculations is not entirely true for this type of microstructure. Nevertheless, we have employed the Eshelby theory for simplicity, in the form of a self-consistent polycrystal deformation model (SCM) [17, 18], using the average elastic constants given in Table 1. As the model utilizes single crystal stiffnesses in the calculations, we have determined “pseudo” values for the BMG (knowing that it is amorphous and does not contain crystalline grains) that result in the correct Young’s modulus and Poisson’s ratio [8] and ensure elastic isotropy.

Table 1. Bulk average (polycrystalline) elastic constants and single crystal stiffnesses of the β phase sample determined from the diffraction data. The “pseudo” single crystal stiffness values given for the BMG are calculated from [8] assuming elastic isotropy.

	E [GPa]	ν	C_{11} [GPa]	C_{12} [GPa]	C_{44} [GPa]	$\frac{2C_{44}}{C_{11} - C_{12}}$
β phase (M5)	59 ± 3	0.37 ± 0.02	92 ± 2	70 ± 2	33 ± 1	3.0
β phase ([8])	63	0.40	-	-	-	-
BMG ([8])	89	0.37	157	92	33	1.0

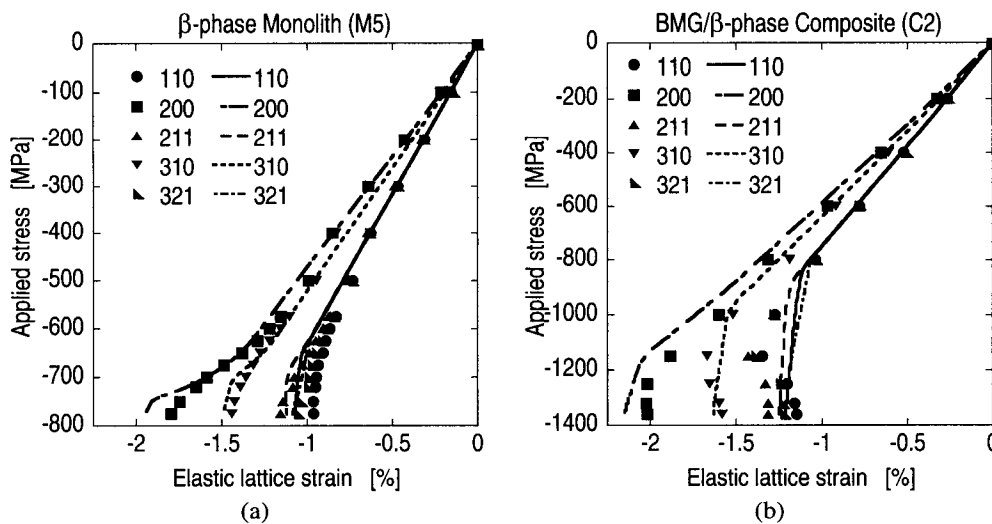


Figure 4. Measured and predicted elastic lattice strains in β phase parallel to the loading axis as a function of applied stress: (a) monolithic β phase (sample M5); (b) β phase/BMG composite (sample C2). Symbols are measured data, lines are SCM predictions.

In the model, the β phase is approximated by spheres, and its plasticity is introduced using the most common slip systems in BCC metals: $\{110\}\langle 111 \rangle$, $\{112\}\langle 111 \rangle$ and $\{123\}\langle 111 \rangle$. The only way of introducing plasticity in the BMG within the current SCM implementation is to assume

“crystal plasticity”, which is of course not appropriate for the glass. However, since we are only interested in the macroscopic behavior of the BMG, we have utilized “crystal plasticity” in it to obtain the effective softening of the BMG as it yields.

The self-consistent model was also used in conjunction with a least squares refinement routine to determine the single crystal stiffnesses of the β phase from the elastic loading slopes of the individual reflections in the *monolith* shown in Fig. 4(a). The results are exhibited in Table 1. The same stiffness data was then used for the β phase in the composite. This approach is similar to the method of Gnäupel-Herold et al. [19], but in their model they do not take into account the angular spread of the measured data due to a finite detector size. Their model only utilizes the nominal direction of the scattering vector, and not the spread in orientations that come from the actual size of the detector. The effect of the angular spread is negligible for isotropic materials, but for anisotropic materials there is going to be a variation over the grains that are suitably oriented for diffraction.

The comparison of the model calculations and the diffraction measurements for both the monolith and composite are shown in Fig. 4. A reasonably good fit in the elastic regime of Fig. 4(b) suggests that the β phase in the composite has approximately the same elastic constants as in monolithic form. In fact, the calculated *in-situ* Young's modulus (defined as the relative change in phase stress vs. phase strain) of the β phase in the composite (62 GPa) is close to that in the monolith (59 GPa).

From the SCM calculations one can also derive the stresses and strains in each phase of the composite. Fig. 5 shows the calculated macroscopic and phase strains versus the applied stress for the composite sample. Here, the axial yield stress of the β phase is seen to be about -690 MPa (which corresponds to -800 MPa applied stress). The von Mises yield stress of the β phase in the composite is about -670 MPa. The BMG matrix, on the other hand yields around -1230 MPa axial stress. In this case the applied macroscopic stress is around -1150 MPa.

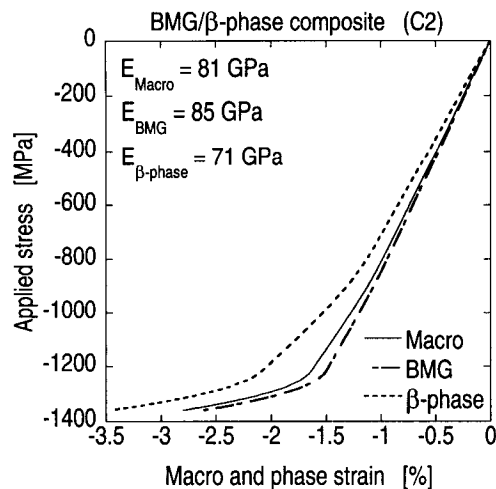


Figure 5. Macroscopic and phase-specific applied stress-strain curves calculated using the self-consistent model [18]. The average *effective* Young's moduli are also shown.

higher in the composite (about -670 MPa). The similarity of both yield strengths and elastic constants of the β phase in both specimens suggests that it has experienced similar heat treatments

Discussion and Conclusions

Despite a non-ideal microstructure, the Eshelby theory (in the form of a self-consistent model) seems to yield reasonable estimates of material properties for the BMG/ β phase composites. The composite stiffness calculated using this theory, 81 GPa, is in good agreement with the literature [8] value of the macroscopic stiffness of the composite, 79 GPa. The effective *in-situ* stiffness of the β phase in the composite calculated using the SCM, 71 GPa, is also close to that measured by diffraction (76 GPa, see Fig. 3(b)). The single crystal stiffness values shown in Table 1 for the monolithic β phase suggest that this phase is highly anisotropic (its anisotropy index was found to be 3.0).

The β phase monolith has a yield strength of about -600 MPa in compression. The *in-situ* yield strength of the β phase is slightly

during processing. This fact alleviates an earlier concern, namely that the mechanical properties of the β phase can vary significantly as a function of heat treatment [20].

The current results clearly show that it is the β phase that yields first during the loading of a BMG/ β phase composite. The load transfer to the BMG matrix that follows and/or the stress concentrations generated at the intersection of slip bands in the β phase and the matrix/particle interface then likely induce multiple shear bands in the BMG matrix as was observed earlier [8]. These shear bands in turn lead to 'plasticity' in the matrix. The details of the micromechanics of this process are still unclear and subject to future investigations.

Acknowledgments

S.Y. Lee was supported by the National Science Foundation (MRSEC program, DMR-0080065) while B. Clausen was partially supported by the Center for Structural Amorphous Metals (ARO grant no. DAAD19-01-0525). This study also benefited from the national user facility at the Manual Lujan, Jr. Center, LANSCE, supported by the Department of Energy under contract W-7405-ENG-36.

References

- [1] C. J. Gilbert, R. O. Ritchie and W. L. Johnson, *Appl. Phys. Lett.*, vol. 71(4), pp. 476-478, 1997
- [2] T. A. Waniuk, J. Schroers and W. L. Johnson, *Applied Physics Letters*, vol. 78(9), pp. 1213-1215, 2001
- [3] A. Masuhr, R. Busch and W. L. Johnson, *Journal of Non-Crystalline Solids*, vol. 250-252, pp. 566-571, 1999
- [4] R.D. Conner, R. B. Dandliker, V. Scruggs and W. L. Johnson, *International Journal of Impact Engineering*, vol. 24, pp. 435-444, 2000
- [5] R. D. Conner, R. B. Dandliker and W. L. Johnson, *Acta Mater.*, vol. 46(17), pp. 6089-6102, 1998
- [6] H. Choi-Yim and W. L. Johnson, *Appl. Phys. Lett.*, vol. 71(26), pp. 3808-3810, 1997
- [7] H. Choi-Yim, R. Busch, U. Köster and W. L. Johnson, *Acta Mater.*, vol. 47(8), pp. 2455-2462, 1999
- [8] F. Szuecs, C. P. Kim and W. L. Johnson, *Acta Mater.* vol. 49, 1507-1513, 2001.
- [9] C. C. Hays, C. P. Kim and W. L. Johnson, *Phys. Rev. Lett.*, vol. 84(13), pp. 2901-2904, 2000.
- [10] B. Clausen, T. Lorentzen, M. A. M. Bourke and M. R. Daymond, *Mat. Sci. & Eng. A*, vol. 259(1), pp. 17-24, 1998
- [11] R. Vaidyanathan, M. A. M. Bourke, D. C. Dunand, *Acta Mater.*, vol. 47(12), pp. 3353-3366, 1999
- [12] H. Choo, M. A. M. Bourke, P. Nash, M. Daymond, N. Shi, *Mat. Sci. & Eng. A*, vol. 264(1-2), pp. 108-121, 1999
- [13] A. C. Wright, *Journal of Non-Crystalline Solids*, vol. 179, pp. 84-115, 1994
- [14] M. A. M. Bourke, J. A. Goldstone, N. Shi, J. E. Allison, M. G. Stout and A. C. Lawson, *Scripta Met.*, vol. 29, pp. 771-776, 1993
- [15] H. M. Rietveld, *J. Appl. Cryst.*, vol. 2, p. 65, 1969
- [16] R. B. Von Dreele, J. D. Jorgensen and C. G. Windsor, *J. Appl. Cryst.*, vol. 15, p. 581, 1982
- [17] B. Clausen, T. Lorentzen and T. Leffers, *Acta Mater.*, vol. 46(9), pp. 3087-3098, 1998
- [18] P. A. Turner and C. N. Tomé, *Acta Mater.*, vol. 42(12), pp. 4143-4153, 1994
- [19] T. Gnäupel-Herold, P. C. Brand and H. J. Prask, *J. Appl. Cryst.*, vol. 31, pp. 929-935 1998
- [20] B. Clausen, E. Üstündag, C. P. Kim, S. Y. Lee, J. C. Hanan, D. W. Brown and M.A.M. Bourke, submitted to *Acta Mater.*, 2002